THE JOURNAL OF
PHYSICAL
CHEMISTRY A
A JOURNAL OF THE AMERICAN CHEMICAL SOCIETY

pubs.acs.org/JPCA Article

Non-Born−Oppenheimer Electronic Structure and Relativistic Effects in the Ground States of BH and BH^+

Published as part of The Journal of Physical Chemistry A special issue "Trygve Helgaker Festschrift".

Saeed Nasiri,* Sergiy Bubin,* and Ludwik Adamowicz*

Cite This: *J. Phys. Chem. A* 2025, 129, 1623−1633 Read Online

ACCESS | Metrics & More | Article Recommendations

ABSTRACT: In this work, we report benchmark variational calculations for the boron monohydride (BH) molecule and its cation (BH^+). The solutions to the nonrelativistic Schrödinger equations for these systems are obtained using a variational method without assuming the Born−Oppenheimer (BO) approximation, which separates electronic and nuclear motions. The ground-state wave functions for both the eight-particle (two nuclei and six electrons) BH molecule and the seven-particle (two nuclei and five electrons) BH^+ ion are expanded in terms of all-particle explicitly correlated Gaussian with prefactors that effectively capture nucleus−nucleus correlation effects. These nonrelativistic non-BO wave functions are used to compute leading-order relativistic corrections to the total energies via perturbation theory, as well as to estimate leading-order quantum electrodynamics (QED) effects. The resulting total, dissociation, and ionization energies of BH represent the most accurate rigorously obtained theoretical values to date.

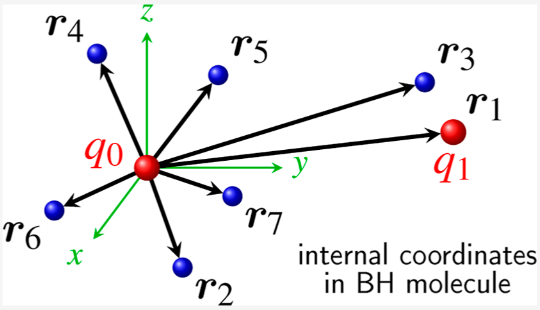

■ INTRODUCTION

Routine first principle quantum-mechanical calculations of molecular systems are typically performed under the Born−Oppenheimer (BO) approximation, which assumes a decoupling of nuclear and electronic motions. Consequently, to determine specific molecular properties, such as geometric structure or spectra, a series of calculations is required for various representative arrangements of the clamped nuclei. These calculations are then used to derive the rovibrational spectrum of the molecule or predict the dynamics of possible chemical reactions the molecule can be involved in. The BO approximation is a bedrock of the present day quantum chemistry. However, in certain cases, decoupling nuclear and electronic motions can introduce hard-to-control inaccuracies or even cause the Born−Oppenheimer approximation to fail entirely. Notable examples include reaction dynamics at the dissociation threshold or interactions with ultrashort laser pulses.

High-precision non-Born−Oppenheimer (non-BO) calculations reported in the literature have been largely limited to the hydrogen molecular ion, hydrogen molecule and its isotopologues. For these one- or two-electron systems it has become possible to calculate the binding energy to an absolutely remarkable precision and achieve excellent agreement with high-resolution spectroscopic measurements.[1−12]

In our works, we have developed ab initio approaches for calculating molecular ground and excited states without assuming the BO approximation, extending these methods to atomic and molecular systems with more than two electrons.[13−25] In these calculations we employ the standard Rayleigh-Ritz variational method. To describe the coupled nuclear−electronic motion we have used all-particle explicitly correlated Gaussian functions (ECGs) that exponentially depend on the squares of the distances between every pair of particles present in the system to expand the system's wave function. Each Gaussian also depends on a set of exponential parameters that are fully optimized in the calculation. The optimization is aided by analytically calculated energy gradient determined with respect to the parameters. This optimization and large number of Gaussian reaching several thousand are key in obtaining results with very high accuracy.

In the non-BO variational calculations we use a Hamiltonian, which is obtained from the laboratory-frame nonrelativistic Hamiltonian by rigorously separating out the center-of-mass motion. The Hamiltonian represents the internal motion of the particles forming the system and it is isotropic. This internal motion occurs in the field of the central potential generated by

Received: November 8, 2024
Revised: January 19, 2025
Accepted: January 23, 2025
Published: February 3, 2025

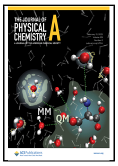

https://doi.org/10.1021/acs.jpca.4c07582

the charge of nucleus, which is chosen to be the reference particle (usually the heavies nucleus).

The calculations presented in this work concern two diatomic systems—the BH molecule and BH^+ molecular ion. The total numbers of particles in the two systems are eight and seven, respectively. The separation of the center-of-mass motion reduces the dimensionality of the BH non-BO Hamiltonian from the original $8 \times 3 = 24$ to $7 \times 3 = 21$. Placing the boron nucleus in the center of the internal coordinate system results in the internal Hamiltonian that represents the motion of seven "pseudo-particles" in the central field of the charge of the boron nucleus. We can call the particles pseudoparticles because, while they have the charges of the original particles, their masses are not the original masses, but the reduced masses. Thus, pseudoparticle 1 is pseudoproton and pseudoparticles 2−7 are pseudoelectrons (see the next section) and the internal wave function has to represent one positively charged particles and six negatively charged particles moving in the central field of a positive charge of the boron nucleus.

In the electronic structure theory, the electron correlation is an effect that needs to be very well represented in the wave. In high-accuracy all-particle non-BO molecular calculations, it is essential to account not only for the electronic correlation with high precision but also to accurately describe the electron−nucleus and nucleus−nucleus correlations effects. The nucleus−nucleus correlation is significantly stronger than the electron−electron correlation due to the substantially larger masses of nuclei compared to the electron mass and due to stronger columbic repulsion between larger charge of the B nucleus. Nuclei tend to avoid each other to a much greater extent than the lighter electrons in their relative motion within the system. As a result, the probability of finding two electrons close to each other in space is much higher than for two nuclei. This, as we discussed before,[13] mandates multiplication of each Gaussian basis function by a product of powers of all internuclear distances. Thus, for a diatomic system, such as the BH molecule, one needs to multiply each Gaussian by powers of the distance between the proton and the boron nucleus, which, as the reference particle, is located in the center of the internal coordinate system (see the next section). Such multipliers are also helpful for generating radial nodes in the non-BO wave function that appear when the system becomes vibrationally excited. The electron−nucleus correlation is also strong, as the electron, particularly the core electrons, follow the moving nuclei very closely. However, as an electron and a nucleus attract, there is no "avoiding" effect in this case. Thus, the exponential parts of the explicitly correlated Gaussian are quite sufficient to represent this correlation effect.

The non-BO ECG calculations carried out for the ground state of the BH molecule in this work, are the largest such calculations ever attempted for a molecular system. Apart from generating very accurate benchmark predictions of such quantities as the BH ionization and dissociation energies, they also provide a demonstration that the non-BO approach can be extended to larger molecular systems. With an increased computational power available and, perhaps, with transitioning to using quantum computers of the future, it may be taken to even larger systems. The increasing size of the molecules that can be calculated with the non-BO ECG approach brings up a possibility to extend the non-BO calculations to study the behavior of larger molecules exposed to static and time-dependent magnetic and electric fields. Some preliminary work in this direction has been recently carried out[26−31] and the results obtained so far indicate that this field may become a very fruitful ground for exploring the role the coupling of the electronic and nuclear motions plays in the phenomena related to the interaction of light and matter.

Furthermore, numerous accurate computational studies have been reported for BH and BH^+ molecules within the BO approximation, with BO corrections calculated at varying levels of accuracy. However, for both molecules, accurate experimental measurements are currently unavailable, making it challenging to assess the reliability of the computed results. It is important to note that none of the previously reported theoretical studies employed a variational approach (see the Results Section), introducing an additional layer of complexity in evaluating their accuracy. In this work, an effort has been made to perform the most precise variational non-BO calculations possible to date. The results of such calculations can serve as a reference for deriving and benchmarking other very accurate postBO calculations.

■ FORMALISM

The approach used in this work to calculate the ground states of diatomic molecules is described in refs 21, 23, and 24. The following nonrelativistic internal Hamiltonian (in atomic units) is used in the present calculations

$$\mathcal{H}_{\mathrm{nr}}^{\mathrm{int}} = -\frac{1}{2}\left(\sum_{i=1}^{n} \frac{1}{\mu_i} \nabla_{\boldsymbol{r}_i}^2 + \sum_{i=1}^{n} \sum_{j \neq i}^{n} \frac{1}{m_0} \nabla_{\boldsymbol{r}_i}' \nabla_{\boldsymbol{r}_j} \right) + \sum_{i=1}^{n} \frac{q_0 q_i}{r_i} + \sum_{i=1}^{n} \sum_{j<i}^{n} \frac{q_i q_j}{r_{ij}}, \tag{1}$$

where $n = N - 1$, N is the total number of particles in the molecule (e.g., the sum of the number of the nuclei and the number of electrons; $N = 8$ for BH and $N = 7$ for BH^+), m_0 is the mass of the reference nucleus (^{11}B, $m_0 = 20\,063.737\,52 m_e$[32]) and $q_0 = +6$ is its charge, q_i, $i = 1, ..., n$, are the charges of the other particles, $\mu_i = m_0 m_i/(m_0 + m_i)$ is the reduced mass of particle i (m_i, $i = 1, ..., n$, are the particle masses), $\boldsymbol{r}_i$, $i = 1, ..., n$ is the distance from particle $n + 1$ to the reference particle, i.e., particle 1, and $\boldsymbol{r}_{ij}$ is the distance between particle $j + 1$ and particle $i + 1$. The prime symbol in eq 1 denotes the matrix/vector transposition. As mentioned in the introduction, the internal Hamiltonian describes n pseudoparticles, which retain their original charges of the actual particles but have their masses replaced by their respective reduced masses, moving in the central field generated by the charge of a reference nucleus. The internal Hamiltonian is rotationally invariant about the origin of the internal coordinate system, resembling an "atom-like" Hamiltonian. Consequently, the eigenfunctions of this Hamiltonian can be classified using atomic symmetry principles. These eigenfunctions, along with their corresponding eigenvalues (energies), encapsulate all modes of the internal molecular motion, including the electronic, vibrational, and rotational modes. In particular, the ground state wave function is spherically symmetric and invariant under 3D rotations.

In order to obtain accurate eigenvalues and wave functions corresponding to rotationless states of Hamiltonian (1), the wave functions are expanded in terms of spherically symmetric all-electron explicitly correlated Gaussian (ECG) basis functions, which have the following form[13]

$$\phi_k = r_1^{m_k} \exp[-\boldsymbol{r}'(A_k \otimes \mathbf{I})\boldsymbol{r}] \tag{2}$$

where r_1 is the distance between the nuclei, m_k is an even integer (in this work, m_k is constrained within the range 0−200 and it is regarded as an integer variational parameter), and A_k is an $n \times n$ real symmetric matrix of the exponential variational parameters. Note that both A_k and m_k are unique and independently tunable for each basis function, which is indicated by index k. Vector $\boldsymbol{r}$ in eq 2 is a $3n$-component vector formed by stacking the internal Cartesian coordinates, $\boldsymbol{r}_i$

$$\boldsymbol{r} = \begin{pmatrix} \boldsymbol{r}_1 \\ \boldsymbol{r}_2 \\ \vdots \\ \boldsymbol{r}_n \end{pmatrix} \tag{3}$$

Let us denote $\boldsymbol{A}_k = A_k \otimes \mathbf{I}$. Matrix $\boldsymbol{A}_k$ and, by extension, A_k, have to be positive definite in order for Gaussian basis function (2) to be square integrable. To ensure positive definiteness of $\boldsymbol{A}_k$ we adopt the following Cholesky-factored form for it: $\boldsymbol{A}_k = (L_k L_k') \otimes \mathbf{I}$, where L_k is a $n \times n$ lower-triangular matrix of real numbers. In this representation, $\boldsymbol{A}_k$ is automatically positive definite for any real-valued L_k. The elements of matrix L_k are variational parameters that are thoroughly optimized in the present calculations. The optimization employs the analytical energy gradient determined with respect to the L_k matrix elements.

ECG basis functions have also been employed in expanding the wave functions of the ground states of B ($2\,^2P$) and B$^+$ ($2\,^2S$) species. Specifically, the following S-type and P-type Gaussian basis functions have been used, respectively[33,34]

$$\phi_k = \exp[-\boldsymbol{r}'(A_k \otimes \mathbf{I})\boldsymbol{r}] \tag{4}$$

$$\phi_k = z_{i_k} \exp[-\boldsymbol{r}'(A_k \otimes \mathbf{I})\boldsymbol{r}] \tag{5}$$

Here z_{i_k} is the z-coordinate of the i_k-th electron. Subscript i_k (the label of the electron in a p state) can vary in the range 1-n and can be considered to be an adjustable integer variational parameter. The parameter is specific for each basis function ϕ_k. Its optimal value is determined variationally when the ECG is first added to the basis set.

All calculations were performed using our in-house parallel computer codes, written in Fortran and utilizing MPI (Message Passing Interface) for communication between parallel processes. It is worth noting that the generation of the basis set for each state—whether for atoms or molecules—is by far the most time-consuming step in these calculations and scales steeply with system size. Among all systems studied here, the eight-particle BH molecule posed the greatest computational challenge, requiring over two years of continuous computing on dozens of CPU cores in a parallel computer system. The largest basis set generated for BH, comprising 5000 ECGs, represents the practical limit of our current computational capacity.

As mentioned in the introduction, the inclusion of $r_1^{m_k}$ factors in Gaussian basis functions (2) for diatomics can be understood by examining the internal Hamiltonian. Specifically, within the framework of $\mathcal{H}_{\mathrm{nr}}$, pseudoparticle 1 represents the proton. As a result, a significant Coulomb repulsion exists between the proton's charge and the charge of the boron nucleus located at the origin of the internal coordinate system. The pair correlation function between these two nuclei, which depends on the internuclear distance r_1, must approach zero rapidly as r_1 approaches zero to satisfy physical constraints. Conversely, for a diatomic molecule in its ground state, this pair correlation function reaches a pronounced peak around $r_1 \approx r_e$, where r_e is the molecule's equilibrium bond length.

The current study focuses on the ground states of the BH and BH$^+$ molecules, as well as the boron atom and its singly charged ion. In constructing the wave functions for each species, we ensure that an appropriate permutational symmetry is enforced. In our approach we adopt the spin-free formalism, as detailed by e.g. Matsen, Pauncz, and Hamermesh.[35−37] A central aspect of this formalism is the construction of a suitable permutational symmetry projector, $\mathcal{Y}$ (the Young operator), which is applied to each basis function. Equivalent terms can also be obtained by pairing spatial basis functions with corresponding spin components and summing over electronic spin coordinates. The Young operator can be presented as a product $\mathcal{Y} = \mathcal{S}\mathcal{A}$, where $\mathcal{S}$ and $\mathcal{A}$ are a symmetrizer over all rows and antisymmetrizer over all columns, respectively, of an appropriate Young tableau. For the ground singlet state of BH molecule, where particles 1 is the B nucleus, particle 2 is the H nucleus (proton), and particles 3−8 are the electrons, the Young operator can be chosen in the following form

$$\mathcal{Y}^{\mathrm{BH}} = \mathcal{S}_{34}\mathcal{S}_{56}\mathcal{S}_{78}\mathcal{A}_{357}\mathcal{A}_{468} \tag{6}$$

where

$$\mathcal{S}_{34} = 1 + \mathcal{P}_{34},\ \mathcal{S}_{56} = 1 + \mathcal{P}_{56},\ \mathcal{P}_{78} = 1 + \mathcal{P}_{78}$$

$$\mathcal{A}_{357} = (1 - \mathcal{P}_{35})(1 - \mathcal{P}_{37} - \mathcal{P}_{57})$$

$$\mathcal{A}_{468} = (1 - \mathcal{P}_{46})(1 - \mathcal{P}_{48} - \mathcal{P}_{68})$$

and $\mathcal{P}_{ij}$ is a transposition operator that permutes the spatial coordinates of the i-th and j-th particle. For the ground doublet state of BH$^+$, where, again, particles 1 and 2 are nuclei, and 3−7 are electrons, the Young operator takes the form

$$\mathcal{Y}^{\mathrm{BH}^+} = \mathcal{S}_{34}\mathcal{S}_{56}\mathcal{A}_{357}\mathcal{A}_{46} \tag{7}$$

with

$$\mathcal{A}_{46} = 1 - \mathcal{P}_{46}$$

In a similar way one can pick appropriate symmetry projectors for the atomic species, B and B$^+$, in which particle 1 is the B nucleus, and particles 2−6 or 2−5 are electrons, respectively

$$\mathcal{Y}^{\mathrm{B}} = \mathcal{S}_{23}\mathcal{S}_{45}\mathcal{A}_{246}\mathcal{A}_{35} \tag{8}$$

$$\mathcal{Y}^{\mathrm{B}^+} = \mathcal{S}_{23}\mathcal{S}_{45}\mathcal{A}_{24}\mathcal{A}_{35} \tag{9}$$

where

$$\mathcal{S}_{23} = 1 + \mathcal{P}_{23},\ \mathcal{S}_{45} = 1 + \mathcal{P}_{45}$$

and

$$\mathcal{A}_{246} = (1 - \mathcal{P}_{24})(1 - \mathcal{P}_{26} - \mathcal{P}_{46}),$$

$$\mathcal{A}_{24} = 1 - \mathcal{P}_{24},\ \mathcal{A}_{35} = 1 - \mathcal{P}_{35}$$

Note that $\mathcal{Y}^{\mathrm{B}}$ corresponds to a doublet electronic state, while $\mathcal{Y}^{\mathrm{B}^+}$ to a singlet state.

The first step in the present calculations is to determine the nonrelativistic, non-BO energies and the corresponding nonrelativistic wave functions. Although these calculations are highly precise and well-converged, they are insufficient for accurate determination of the total, ionization, and dissociation energies when compared to state-of-the-art spectroscopic measurements. To achieve a closer agreement with experimental data, it is essential to include relativistic and quantum electrodynamics (QED) corrections in the calculations. This is done by expanding the total energy of the system as a series in powers of the fine-structure constant, α[38,39]

$$E_{\text{tot}} = E_{\text{nr}} + \alpha^2 E^{(2)}_{\text{rel}} + \alpha^3 E^{(3)}_{\text{QED}} + \dots \tag{10}$$

where E_{nr} is the nonrelativistic energy of the considered state of the system, the second term, $\alpha^2 E^{(2)}_{\text{rel}}$, represents the leading-order relativistic correction, the third term $\alpha^3 E^{(3)}_{\text{QED}}$ represents the leading-order QED correction, and so on. Each of these terms is evaluated as an expectation value of a certain effective Hamiltonian. In our calculations, quantity $E^{(2)}_{\text{rel}}$ in eq 10 is the expectation value of the Breit−Pauli Hamiltonian, $\mathcal{H}_{\text{rel}}$, corresponding to the ground state of BH, BH$^+$, B, and B$^+$.[40,41] In the present work, $\mathcal{H}_{\text{rel}}$, before it is used in the calculations, is expressed in terms of the internal coordinates. The mass−velocity ($\mathcal{H}_{\text{MV}}$), Darwin ($\mathcal{H}_{\text{D}}$), orbit−orbit interaction ($\mathcal{H}_{\text{OO}}$), spin−spin Fermi contact interaction ($\mathcal{H}_{\text{SS}}$), and spin−orbit interaction ($\mathcal{H}_{\text{SO}}$) are included in $\mathcal{H}_{\text{rel}}$

$$\mathcal{H}_{\text{rel}} = \mathcal{H}_{\text{MV}} + \mathcal{H}_{\text{D}} + \mathcal{H}_{\text{OO}} + \mathcal{H}_{\text{SS}} + \mathcal{H}_{\text{SO}} \tag{11}$$

The explicit expressions for the corresponding effective operators in the internal coordinates are as follows[42,43]

$$\mathcal{H}_{\text{MV}} = -\frac{1}{8}\left[\frac{1}{m_0^3}\Big(\sum_{i=1}^{n} \nabla_{\boldsymbol{r}_i}\Big)^4 + \sum_{i=1}^{n} \frac{1}{m_i^3}\nabla^4_{\boldsymbol{r}_i}\right] \tag{12}$$

$$\begin{aligned}\mathcal{H}_{\text{D}} = -\frac{\pi}{2}\Big[&\sum_{i=2}^{n} \frac{q_0 q_i}{m_i^2}\delta(\boldsymbol{r}_i) + \\ &\sum_{i=2}^{n} \frac{q_1 q_i}{m_i^2}\delta(\boldsymbol{r}_{1i}) + \sum_{i,j=2}^{n} \frac{q_i q_j}{m_i^2}\delta(\boldsymbol{r}_{ij})\Big],\end{aligned} \tag{13}$$

$$\begin{aligned}\mathcal{H}_{\text{OO}} =& \\ &-\frac{1}{2}\sum_{i=1}^{n}\sum_{j=1}^{n}\frac{q_0 q_j}{m_0 m_j}\left[\frac{1}{r_j}\nabla'_{\boldsymbol{r}_i}\nabla_{\boldsymbol{r}_j} + \frac{1}{r_j^3}\boldsymbol{r}'_j(\boldsymbol{r}'_j\nabla_{\boldsymbol{r}_i})\nabla_{\boldsymbol{r}_j}\right] \\ &+\frac{1}{2}\sum_{i=1}^{n}\sum_{j>i}^{n}\frac{q_i q_j}{m_i m_j}\left[\frac{1}{r_{ij}}\nabla'_{\boldsymbol{r}_i}\nabla_{\boldsymbol{r}_j} + \frac{1}{r_{ij}^3}\boldsymbol{r}'_{ij}(\boldsymbol{r}'_{ij}\nabla_{\boldsymbol{r}_i})\nabla_{\boldsymbol{r}_j}\right],\end{aligned} \tag{14}$$

and

$$\mathcal{H}_{\text{SS}} = -\frac{8\pi}{3}\sum_{\substack{i,j=2\\ j>i}}^{n}\frac{q_i q_j}{m_i m_j}(\boldsymbol{s}'_i\boldsymbol{s}_j)\delta(\boldsymbol{r}_{ij}) \tag{15}$$

where in the last expression, $\boldsymbol{s}_i$ denotes the spin operator of the i-th pseudoparticle. For the states of systems considered in this work

$$\langle \boldsymbol{s}'_i\boldsymbol{s}_j\delta(\boldsymbol{r}_{ij})\rangle_{\boldsymbol{r},\boldsymbol{\sigma}} = -\frac{3}{4}\langle\delta(\boldsymbol{r}_{ij})\rangle_{\boldsymbol{r}}$$

where the subscripts $\boldsymbol{r}$ and $\boldsymbol{\sigma}$ stand for averaging over the spatial and spin coordinates, respectively. Note that expressions (12) and (14) above are general, while (13) and (15) are given specifically for diatomic molecules, where particles 1 and 2 are nuclei. In the case of atomic species all summation indices in them should start with 1 and the second sum in (13) is dropped.

The relativistic corrections for a particular state are calculated as the expectation values of the above operators using the state's nonrelativistic non-BO wave function. At the lowest-order approximation, the spin−orbit interaction that gives rise to the fine structure splitting is obtained as a sum of two terms. The first term is an expectation value of the following operator

$$\begin{aligned}\mathcal{H}_{\text{SO}} = \mathcal{H}_{\text{SO1}} + \mathcal{H}_{\text{SO2}} =& \\ &+ i\sum_{i=1}^{n}\frac{q_0 q_i}{2m_i}\left(\frac{1}{m_i} + \frac{2}{m_0}\right)\frac{\boldsymbol{s}'_i}{r_i^3}(\boldsymbol{r}_i \times \nabla_{\boldsymbol{r}_i}) \\ &+ i\sum_{\substack{i,j=1\\ j\neq i}}^{n}\Bigg\{\frac{q_0 q_i}{m_0 m_i}\frac{\boldsymbol{s}'_i}{r_i^3}(\boldsymbol{r}_i \times \nabla_{\boldsymbol{r}_j}) \\ &- i\frac{q_i q_j}{2m_i}\frac{\boldsymbol{s}'_i}{r_{ij}^3}\left[(\boldsymbol{r}_i - \boldsymbol{r}_j) \times \left(\frac{1}{m_i}\nabla_{\boldsymbol{r}_i} - \frac{2}{m_j}\nabla_{\boldsymbol{r}_j}\right)\right]\Bigg\},\end{aligned} \tag{16}$$

$\mathcal{H}_{\text{SO}_1}$ and $\mathcal{H}_{\text{SO}_2}$ are the one- and two-electron parts of the $\mathcal{H}_{\text{SO}}$ operator, respectively. They are often referred to as the spin−orbit and spin−other−orbit interactions, respectively. In the lowest order, the fine-structure splitting is calculated as the expectation value of $\mathcal{H}_{\text{SO}}$ using the nonrelativistic wave function obtained in the variational calculation using the internal Hamiltonian (1). Similarly to the nonrelativistic Hamiltonian, the Hamiltonian for calculating the spin−orbit interaction also depends on the nuclear mass m_0.[44] In the limit of an infinite nuclear mass, the Hamiltonian reduces to a sum of the standard spin−orbit and spin−other−orbit interaction operators. Therefore, the recoil corrections to the spin−orbit interaction are automatically included in the calculations. To obtain the leading-order energy correction the expectation value of $\mathcal{H}_{\text{SO}}$ is multiplied by α^2. The next-order effect contributing to the fine structure splitting is due to anomalous magnetic moment (AMM) of the electron. This term is given by the expectation value of the following Hamiltonian

$$\begin{aligned}\mathcal{H}_{\text{AMM}} = \mathcal{H}_{\text{AMM}_1} + \mathcal{H}_{\text{AMM}_2} =& \\ &+ i\sum_{i=1}^{n}\frac{q_0 q_i}{2m_i^2}\frac{\boldsymbol{s}'_i}{r_i^3}(\boldsymbol{r}_i \times \nabla_{\boldsymbol{r}_i}) \\ &+ i\sum_{\substack{i,j=1\\ j\neq i}}^{n}\frac{q_i q_j}{2m_i}\frac{\boldsymbol{s}'_i}{r_{ij}^3}\left[(\boldsymbol{r}_i - \boldsymbol{r}_j) \times \left(\frac{1}{m_i}\nabla_{\boldsymbol{r}_i} - \frac{1}{m_j}\nabla_{\boldsymbol{r}_j}\right)\right].\end{aligned} \tag{17}$$

The $\mathcal{H}_{\text{AMM}}$ term is multiplied by $2\kappa\alpha^2$, where $\kappa = 1.15965218128 \times 10^{-3}$ is the electron magnetic moment anomaly.[45] The resulting contribution of this effect is proportional to α^3. It should be noted that operator $\mathcal{H}_{\text{AMM}}$ is obtained within the infinite-nuclear-mass (INM) approximation and, thus, does not contain any recoil corrections. For more details see our previous works.[25,42,43,46]

The largest contribution to the leading QED correction comes from the term containing the Bethe logarithm, ln k_0.[47,48] In our previous works,[24,25] we discussed the challenges involved in computing this QED correction. The main difficulty lies in accurately determining the term involving ln k_0. To our knowledge, despite of proposing some efficient algorithms to

Table 1. Convergence of the Nonrelativistic Variational Nnon-BO Energy (E_{nr}) and the Expectation Values of the Mass−Velocity Hamiltonian ($\mathcal{H}_{\mathrm{MV}}$), Orbit−Orbit Hamiltonian ($\mathcal{H}_{\mathrm{OO}}$), and One- and Two-Electron Dirac δ-Functions for the Ground State of BH, BH$^+$, B, and B$^+$ Species[a]

basis	E_{nr}	$\langle \mathcal{H}_{\mathrm{MV}} \rangle$	$\langle \mathcal{H}_{\mathrm{OO}} \rangle$	$\langle \delta(\mathbf{r}_{\mathrm{B-e}}) \rangle$	$\langle \delta(\mathbf{r}_{\mathrm{H-e}}) \rangle$	$\langle \delta(\mathbf{r}_{\mathrm{e-e}}) \rangle$
BH						
2000	−25.28028	−686.7	−1.63507	11.836	0.07512	0.23777
3000	−25.28115	−688.1	−1.63569	11.864	0.07571	0.23760
4000	−25.28152	−688.8	−1.63546	11.878	0.07600	0.23747
5000	−25.28173	−690.2	−1.63598	11.906	0.07626	0.23722
∞	−25.28222 ± 0.00049	−693.58 ± 3.35	−1.63643 ± 0.00045	11.953 ± 0.047	0.07683 ± 0.00057	0.23686 ± 0.00036
BH$^+$						
4000	−24.921403	−689.49	−1.66596	14.278	0.07929	0.35490
6000	−24.921592	−689.65	−1.66847	14.283	0.07972	0.35427
8000	−24.921661	−689.90	−1.66960	14.289	0.07991	0.35404
10 000	−24.921692	−690.31	−1.66984	14.300	0.08002	0.35386
∞	−24.921732 ± 0.000040	−690.94 ± 0.62	−1.67062 ± 0.00078	14.315 ± 0.015	0.08051 ± 0.00049	0.35318 ± 0.00068
B						
10 000	−24.65262582	−693.22236	−1.14155411	14.37082420		0.353798253
12 000	−24.65262607	−693.22239	−1.14155388	14.37082516		0.353798300
14 000	−24.65262621	−693.22242	−1.14155359	14.37082554		0.353798332
16 000	−24.65262633	−693.22201	−1.14155307	14.37082591		0.353798362
∞	−24.65262651 ± 0.00000018	−693.22178 ± 0.00023	−1.14155269 ± 0.00000038	14.37082686 ± 0.00000095		0.353798434 ± 0.000000072
B$^+$						
2000	−24.3476411905	−699.696603	−1.569089083	18.12384038		0.596231528
3000	−24.3476412839	−699.695582	−1.569088333	18.12384086		0.596231618
4000	−24.3476413124	−699.695601	−1.569088270	18.12384104		0.596231630
5000	−24.3476413184	−699.695564	−1.569088233	18.12384108		0.596231636
∞	−24.3476413209 ± 0.0000000025	−699.695536 ± 0.000028	−1.569088178 ± 0.000000055	18.12384135 ± 0.00000027		0.596231716 ± 0.000000070
H						
exact	−0.499727839712	−0.623640309	−0.000543728	0.318309886		

[a] Results obtained with basis sets of different size are shown along with the extrapolated values. The numbers in parentheses are estimated uncertainties of the extrapolation due to the basis set truncation. All values are in a.u.

calculate $\ln k_0$ term[49,50] for atomic or molecular species, no direct calculation of $\ln k_0$ has been reported for the B, BH, and BH^+ species using ECG basis functions. Recently, Lesiuk and Lang[51] reported a $\ln k_0$ value for the B atom obtained using the mean-field (MF) approximation. Their reported value of 6.339 is significantly larger than the estimate provided by Puchalski et al.,[52] which is 6.195(5). Further comparison of the reported $\ln k_0$ values for lithium and beryllium with those obtained using the ECG/Hy methods reveals a systematic overestimation of the values in the MF calculations. For lithium, $\ln k_0(\mathrm{Li, Hy}) = 5.17817$ and $\ln k_0(\mathrm{Li, MF}) = 5.194$, while for beryllium, $\ln k_0(\mathrm{Be, ECG}) = 5.750\,46$ and $\ln k_0(\mathrm{Be, MF}) = 5.763$. It is well established that the dominant contribution to $\ln k_0$ in atoms originates from the inner-shell electrons. As a result, the value estimated by Puchalski et al.[52] is adopted in the present calculations. Therefore, the following approximate expression for the effective leading-order QED Hamiltonian can be adopted

$$\mathcal{H}^{(3)}_{\mathrm{QED}} \approx \frac{4q_0}{3}\left(\frac{19}{30} - 2\ln\alpha - \ln k_0(\mathrm{B/B^+})\right)\sum_{i=2}^{n}\langle\delta(\boldsymbol{r}_{\mathrm{B}-i})\rangle + \frac{4q_{\mathrm{H}}}{3}\left(\frac{19}{30} - 2\ln\alpha - \ln k_0(\mathrm{H})\right)\sum_{i=2}^{n}\langle\delta(\boldsymbol{r}_{\mathrm{H}-i})\rangle, \quad (18)$$

where $\ln k_0(\mathrm{B}) = 6.195(5)$,[52] $\ln k_0(\mathrm{B^+}) = 6.1944(9)$,[53] and $\ln k_0(\mathrm{H}) = 2.984\,129$[54] are the Bethe-logarithm values, and $\boldsymbol{r}_{\mathrm{B}-i}$ and $\boldsymbol{r}_{\mathrm{H}-i}$ stand for the 3D Dirac delta functions that depend on the nucleus−electron distances.

Expressions (11) and (18) contain singular operators.

These are the squares of the linear momentum squares and the Dirac delta functions. The expectation values of these operators are known to exhibit slower convergence with the basis size in the Rayleigh-Ritz variational method compared to the case of nonsingular operators (e.g., the nonrelativistic Hamiltonian). In this work, when evaluating such expectation values for atomic species B and B^+ we adopted a regularization scheme (commonly referred to as "Drachmanization"[55]) as described in refs 56 and 57. However, for the molecular species, BH and BH^+, these expectation values are evaluated directly because the calculation of needed integrals in the case of basis functions (2) is too involved.

■ RESULTS

Table 1 presents the calculated total non-BO nonrelativistic energies, the leading relativistic corrections, and several key expectation values for the ground states of the BH, BH^+, B, B^+, and H species. As previously mentioned, BH is the largest system studied to date using all-particle ECG basis functions.

In addition to the values computed using varying basis set sizes, Table 1 also includes energies and other expectation values extrapolated to the infinite basis set limit. Over the past two decades, our experience in working with ECG calculations has shown that extending the basis set by linearly increasing multiples of a certain number of functions often results in energy increments that resemble a geometric progression. Consequently, we extrapolate to the infinite basis set limit using a geometric progression approximation. For more details, please see our previous publication.[70] The extrapolated values are presented alongside their estimated uncertainties. It can be seen that different expectation values exhibit different levels of convergence. For instance, the estimated accuracy of the computed nonrelativistic energy of BH is approximately half of a millihartree, whereas the estimated uncertainty for B^+ is around 2.5 nanohartree. Consequently, when evaluating the ionization or dissociation energy, the primary contribution to the total error is expected to originate from the larger system—BH.

Table 2. Expectation Values (in a.u.) of $\mathcal{H}_{\mathrm{SO}}$ and $\mathcal{H}_{\mathrm{AMM}}$ in the Ground State of the Boron Atom[a]

basis	$\langle\mathcal{H}_{\mathrm{SO}}\rangle$	$\langle\mathcal{H}_{\mathrm{AMM}}\rangle$
10 000	0.43482914	0.50591393
12 000	0.43482946	0.50591419
14 000	0.43482958	0.50591446
16 000	0.43482991	0.50591456
∞	0.43483037 ± 0.00000046	0.50591486 ± 0.00000030

[a] The numbers in parentheses are estimated uncertainties due to the basis truncation.

Table 2 shows the expectation values of the $\mathcal{H}_{\mathrm{SO}}$ and $\mathcal{H}_{\mathrm{AMM}}$ Hamiltonians for the spin−orbit term. These values are shown exclusively for the boron atom (in 2^2P state) as the spin−orbit interaction is absent in all other systems. The results exhibit convergence up to eight decimal places. Recently, we investigated the fine structure of the 2^2P states of the boron atom, achieving the most accurate calculations reported to date (see ref 71 for further details).

The basis sets used to obtain the results in Tables 1 and 2 were generated in a process that begins with a small set of Gaussian functions. The nonlinear parameters of these functions are selected using a mix of random and physically motivated choices followed by optimization. The basis set is then systematically expanded over several steps. In each step, new Gaussian functions are added and variationally optimized using a procedure that employs the analytical energy gradient. The enlargement and subsequent optimization are performed using a one-function-at-a-time approach. After a newly added function is optimized, it is checked for linearly dependency (within a predefined threshold) with the existing functions in the set. If no linear dependencies are detected, the function is retained in the basis set. As mentioned previously, both the L_k matrix elements and the m_k powers in the r_1 pre-exponential factors are subject to the optimization. However, because m_k's can only take even integers, their optimization is performed only once when the corresponding functions are first included in the basis. This optimization is conducted using a stochastic search with a predefined number of trials. The range of the allowed values for m_k's is set to 0−200. After a certain small number of Gaussian are added to the basis set, the nonlinear parameters of all functions in the set generated so far are reoptimized, again using a one-function-at-a-time approach. In this reoptimization, only the L_k matrix elements are varied, while the m_k values remain fixed.

Table 3 compares of the nonrelativistic energies of BH and BH^+ obtained in the current work with the most accurate values reported in the literature. All previous studies were performed within the BO approximation, excluding diagonal BO (DBO) and nonadiabatic corrections. However, Valeev et al.[60] and Martin[72] demonstrated that both DBO and nonadiabatic corrections are fairly significant for the BH molecule, impacting not only the nonrelativistic energy but also other properties,

Table 3. Comparison of the Nonrelativistic Non-BO Energies of the BH and BH^+ Molecules Obtained in This Work With the Most Accurate Values of the Nonrelativistic BO + ZPE + DBO Energy Available in the Literature (All in a.u.)[a,b]

method/basis	E_{nr}
BH	
this work, 5000 ECGs	−25.28173
this work, extrapolated	−25.28222 ± 0.00049
CCSD(T)/aug-cc-pV5Z[61]	−25.229208
CCSDT/d-aug-cc-pV5Z[58]	−25.280516
MR-CI/d-aug-cc-pV5Z[58]	−25.280444
MR-CI + Q/d-aug-cc-pV5Z[58]	−25.280646
BH^+	
this work, 10 000 ECGs	−24.921692
this work, extrapolated	−24.921732 ± 0.000040
QCISD(T)/cc-pV(T+d)Z[62]	−24.866935

[a] The ZPE values for BH and BH^+ were taken from refs 58 and 59, respectively. The DBO correction is only added to the BH molecule's energy. The correction is taken from ref 60. [b] The DBO correction has not been found in the literature and, thus, it is not added to the BO energy of BH^+. However, as this correction is positive, the total energy value without the correction being higher than the non-BO energy indicates that the quality of the non-BO result is significantly higher than the BO result.

Table 4. Ionization Energies (IE) of 11BH Obtained in This Work at the Nonrelativistic Level of Theory and Then by Including the Leading Relativistic and QED Corrections[a]

basis (BH)	basis (BH^+)	IE_{nr}	IE_{nr+rel}	$IE_{nr+rel+QED}$
2000	4000	78 113	78 738	78 739
3000	6000	78 913	78 914	78 915
4000	8000	79 026	78 987	78 987
5000	10 000	79 019	79 028	79 028
∞	∞	79 026 ± 7	79 081 ± 53	79 081 ± 53
experiment, ref 63				78 800 ± 403
experiment, ref 64				78 800
experiment, ref 59				79120.3 ± 0.1

[a] Available experimental IE values are also shown for comparison. All values are in cm^{-1}.

such as the bond length. For example, Valeev et al. reported a DBO correction of 369.97 cm^{-1} for BH calculated at the CISD/aug-cc-pVTZ level of theory. In this study, we incorporate the DBO correction[60] and the zero-point energy (ZPE)[58] into the reported BO energy values to facilitate a more direct comparison with our non-BO energies (see Table 3). However, the BO + ZPE + DBO energies still do not include the nonadiabatic corrections. These corrections are automatically included to infinite order in our variational non-BO nonrelativistic energy values. With this in mind, for BH, the present total energy obtained using 5000 ECGs is lower and, due to the nature of the variational method, is more accurate than those calculated at the CCSDT/d-aug-cc-pV5Z and MR-CI + Q/d-aug-cc-pV5Z levels of theory.[58]

Both methods lack the variational principle, which means they cannot ensure that the energy is a strict upper bound to the true value. For BH^+, the available computational data are very limited, with the most accurate values sourced from the NIST Computational Chemistry Comparison and Benchmark Database.[62] Additionally, as the DBO correction has not been reported for this ion yet, the reference BO energy value presented in the table for comparison with our non-BO energy does not include the DBO correction. As the DBO correction, which is calculated as the expectation value of the kinetic energy operator for the nuclei using the electronic wave function, has a positive value, its addition to the result shown in the table would make this result even less negative and higher than our non-BO energy. This confirms that our present nonrelativistic BH energy is significantly more accurate than the best energy obtained within the BO approximation.

The ionization energies (IE) calculated using the nonrelativistic non-BO energies (E_{nr}), the nonrelativistic non-BO energies plus the leading relativistic corrections (E_{nr+rel}), and the nonrelativistic non-BO energies plus the leading relativistic and QED corrections ($E_{nr+rel+QED}$) are shown in Table 4. In addition to the non-BO values calculated in the present work, some of the values derived from experimental data are also shown in the table. It can be seen that the obtained IE value using the nonrelativistic energies (IE_{nr} = 79 026 (7) cm^{-1}) is less accurate compared to the ones obtained with the inclusion of relativistic corrections (IE_{nr+rel} = 79 081 (53) cm^{-1}). In computing the IE, the QED correction has an almost negligible contribution. IE_{nr+rel} and $IE_{nr+rel+QED}$ are virtually the same within the estimated uncertainty. It should be emphasized, however, that the QED correction calculated in this work using expression (18) is a very crude estimate only. It could be improved in future studies if efficient algorithms for evaluating the Bethe logarithm for diatomic molecules are developed. In addition to the ionization energies calculated in this work, Table 4 shows three experimental values. The reported uncertainty for the first experiment[63] is rather large −403 cm^{-1}. Although the uncertainty is not reported for the second measurement,[64] a similar error magnitude as for the first experimental value (approximately 400 cm^{-1}) can be expected. The most recent experimental value from ref 59 appears to be considerably more accurate than the other two and aligns well with the value obtained in the present work (79 081 cm^{-1}), falling within the estimated theoretical uncertainty of 53 cm^{-1}. This theoretical uncertainty primarily arises from basis set truncation error. As shown in Table 1, a significant contribution to the uncertainty comes from the nonrelativitic BH energies, suggesting that a larger number of basis functions would be required for improved accuracy in the calculations. An even larger contribution to the overall uncertainty, however, originates from the limited accuracy in evaluating relativistic corrections for BH and BH^+. Future advancements in the evaluation of expectation values for singular operators will likely require the implementation of regularization techniques, such as integral transformation,[73] plain capping,[74] integral transformation of inverse interparticle distances,[75] or the regularization algorithm proposed by Rácsai.[76] In Table 5 presents the calculated dissociation energies (D) for both BH and BH^+ alongside the available experimental and theoretical values. From the data, it is evident that both the relativistic and QED corrections are again crucial for obtaining an accurate value of the dissociation energy in the calculations. For instance, in the case of the BH molecule purely nonrelativistic dissociation energy D_{nr} = 28 480 (86) cm^{-1} differs notably from the values obtained with including the relativistic (D_{nr+rel} = 28 464 (82) cm^{-1}) and QED ($D_{nr+rel+QED}$ = 28 407 (87) cm^{-1}) corrections. The uncertainty of the available experimental dissociation energies is also quite significant—approximately 150 cm^{-1} for BH and likely even higher one for

Table 5. Comparison of the Dissociation Energies (D) of ^{11}BH and ^{11}BH$^+$ Obtained in This Work With the Most Accurate Theoretical Values and Experimental Measurements[a]

		D_{nr}	$D_{\mathrm{nr+rel}}$	$D_{\mathrm{nr+rel+QED}}$
		BH		
basis (BH)	basis (B)			
2000	10 000	28 077	28 062	28 001
3000	12 000	28 267	28 253	28 192
4000	14 000	28 348	28 335	28 273
5000	16 000	28 394	28 382	28 320
∞	∞	28 480 ± 86	28 464 ± 82	28 407 ± 87
CCSD(T), ref 61[b]		28 400		
CCSD(T), ref 61[c]		28 505		
CCSD(T), ref 61[d]		28 575		
MR-ACPF, ref 65[e]		27 428		
MR-DCI, ref 66[f]		28 859		
CCSDT, ref 58[g]		29 653		
experiment, ref 67				28 850 ± 150
experiment, ref 64				27 584
experiment, ref 68				28 505 ± 175
		BH$^+$		
basis (BH$^+$)	basis (B$^+$)			
4000	2000	16 249	16 224	16 164
6000	3000	16 290	16 265	16 205
8000	4000	16 305	16 281	16 220
10 000	5000	16 312	16 288	16 227
∞	∞	16 322 ± 10	16 298 ± 10	16 237 ± 10
MR-CI, ref 69[h]		15 958		
experiment, ref 64				15 728

[a] All values are in cm^{-1}. [b] Value obtained with aug-cc-pV5Z basis set. [c] Value obtained by extrapolating CCSD(T)/aug-cc-pVnZ (n = 2−5) calculations to the infinite basis set limit using the equation $E(n) = E(\infty) + B\ \exp(-C\ n)$. [d] Value obtained by extrapolating CCSD(T)/aug-cc-pVnZ (n = 2−5) calculations to the infinite basis set limit using the equation $E(l_{\max}) = E(\infty) + A/(l_{\max} + 0.5)^4$. [e] Multireference averaged coupled-pair functional (MR-ACPF) method. The computed values with aug-cc-pVnZ (n = 4−7) basis sets were extrapolated to infinite basis set limit. [f] Multireference single and double excitations configuration interaction (MR-DCI) level of theory with VQZ basis set of Dunning. [g] The d-aug-cc-pV5Z and cc-pV5z basis sets have been used for Boron and hydrogen, respectively. [h] Valence internally contracted multireference configuration interaction (MR-CI) method with aug-cc-pV6Z basis set.

BH$^+$. While three experimental values of D are reported for BH, they are not in good agreement with one another, and only two fall within the stated uncertainties. For BH$^+$, there is a single experimental value with an unknown uncertainty. For both species, lack of precise experimental values makes it challenging to perform a reliable comparison with our results and to assess the accuracy of our computations. Additionally, all previous theoretical values in the literature have been obtained within the BO approximation without considering DBO and nonadiabatic corrections, introducing another layer of uncertainty to the comparison. As mentioned before, both of the aforementioned corrections are significant for BH and likely important for BH$^+$. Nevertheless, the computed D_{nr} value for BH in this work shows reasonable agreement with the other theoretical values (see Table 5).

The non-BO nonrelativistic wave functions obtained for ^{11}BH have been used to calculate the expectation values for the interparticle distances and their squares. These results are presented in Table 6. Alongside the values calculated in this work, the table also includes related quantities derived from BO calculations, such as r_e and r_0. Due to the explicit inclusion of the electron−nuclear coupling in the non-BO calculations, the agreement between the values obtained here and those from previous BO calculations is not particularly good. This observation aligns with the conclusions from the earlier BO studies,[58,61,69] where it was noted that adiabatic and nonadiabatic effects are significant when calculating properties of diatomic systems.

Lastly, in Figure 1, we present the nucleus−nucleus pair correlation functions calculated for the ground states of BH and BH$^+$ using the non-BO wave functions expanded in the largest basis sets generated in this work. As shown, the density of the proton in both systems is localized around the respective average distances. However, for BH, the density is slightly less sharply peaked and broader compared to BH$^+$.

■ CONCLUSIONS

In this work we report the most accurate non-Born−Oppenheimer calculations performed to date for the ground states of ^{11}BH and ^{11}BH$^+$. The calculations employ all-particle explicitly correlated Gaussian basis functions, with extensive variational optimization of the nonlinear parameters for each state. This optimization is carried out using a procedure that utilizes the analytic energy gradient with respect to the Gaussian parameters. The resulting nonrelativistic non-BO wave functions are used to calculate the leading relativistic and QED corrections. The corrections are added to the non-BO nonrelativistic energies and the results are used to calculate the ^{11}BH dissociation energy, as well as the ^{11}BH ionization energy. The obtained results fall within the uncertainties of the available experimental data, providing a reliable benchmark for future theoretical studies. Additionally, these results offer valuable

Table 6. Average Interparticle Distances and Their Squares (All in a.u.) Obtained for ^{11}BH and ^{11}BH$^+$ in Present Non-BO Calculations[a]

quantity	method	BH	BH$^+$
$\langle r_{\text{Li-H}} \rangle$		2.36249 ± 0.00011	2.311195 ± 0.000055
$\langle r_{\text{Li-e}} \rangle$		1.54787 ± 0.00078	1.297965 ± 0.000030
$\langle r_{\text{H-e}} \rangle$		2.55435 ± 0.00069	2.312213 ± 0.000073
$\langle r_{\text{e-e}} \rangle$		2.50326 ± 0.00157	2.106729 ± 0.000066
$\langle r^2_{\text{Li-H}} \rangle$		5.6090 ± 0.0006	5.36843 ± 0.00025
$\langle r^2_{\text{Li-e}} \rangle$		3.7754 ± 0.0069	2.72733 ± 0.00023
$\langle r^2_{\text{H-e}} \rangle$		7.9251 ± 0.0056	6.29142 ± 0.00042
$\langle r^2_{\text{e-e}} \rangle$		8.0283 ± 0.0138	5.70205 ± 0.00047
r_e	CCSD(T), ref 61[b]	2.3295	
r_e	MR-ACPF, ref 65[c]	2.3284 ± 0.00019	
r_e	MR-CI, ref 69[d]		2.27542
r_e	CCSDT, ref 58[e]		2.3251
r_e	fitting, ref 64[e]	2.3289	2.29545
r_e	fitting, ref 59[f]		2.275174 ± 0.000013
r_0	MR-ACPF, ref 65[g]	2.36158	

[a] For comparison we also show BO equilibrium bond lengths, r_e, obtained in theoretical calculations before, as well as a value derived from the experiment. [b] Values obtained with aug-cc-pv5Z basis set. [c] Multireference averaged coupled-pair functional (MR-ACPF) method. The computed values with aug-cc-pVnZ (n = 4−7) basis sets were extrapolated to the infinite basis set limit. [d] Valence internally contracted multireference configuration interaction (MR-CI) method with aug-cc-pV6Z basis set. [e] The d-aug-cc-pV5Z and cc-pV5Z basis sets have been used for Boron and hydrogen, respectively. [f] This value was extracted from experimental data using a fitting procedure. [g] The vibrationally averaged value ($r_0 \equiv \langle r \rangle_0$) was calculated in this work using the potential energy curve reported in ref 65. The calculations were performed with the LEVEL code.[77]

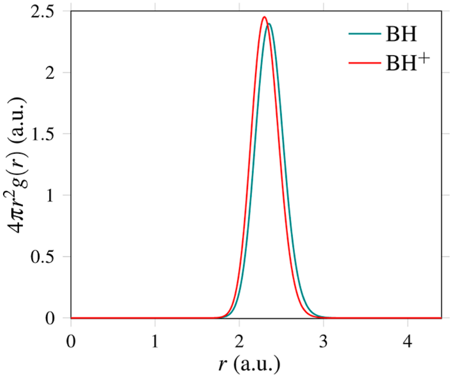

Figure 1. Nucleus−nucleus pair correlation functions for the ground states of BH and BH$^+$ calculated using the largest ECG basis sets generated in this work.

reference points for future spectroscopic measurements of BH and BH$^+$.

■ AUTHOR INFORMATION

Corresponding Authors

Saeed Nasiri − *Department of Physics, Nazarbayev University, Astana 010000, Kazakhstan*; Email: saeed.nasiri@nu.edu.kz

Sergiy Bubin − *Department of Physics, Nazarbayev University, Astana 010000, Kazakhstan*; Email: sergiy.bubin@nu.edu.kz

Ludwik Adamowicz − *Department of Chemistry and Biochemistry and Department of Physics, University of Arizona, Tucson, Arizona 85721, United States*; orcid.org/0000-0001-9557-0484; Email: ludwik@arizona.edu

Complete contact information is available at: https://pubs.acs.org/10.1021/acs.jpca.4c07582

Notes

The authors declare no competing financial interest.

■ ACKNOWLEDGMENTS

This work has been partially supported by the National Science Foundation (grant no. 1856702) and Nazarbayev University (FDCRGP grant “Precise atomic structure calculations with explicitly correlated functions”). Authors acknowledge the use of the high performance computational resources provided by Nazarbayev University Research Computing.

■ REFERENCES

(1) Korobov, V. I.; Koelemeij, J. C. J.; Hilico, L.; Karr, J.-P. Theoretical Hyperfine Structure of the Molecular Hydrogen Ion at the 1 ppm Level. *Phys. Rev. Lett.* **2016**, *116*, 053003.

(2) Korobov, V. I.; Hilico, L.; Karr, J.-P. Fundamental Transitions and Ionization Energies of the Hydrogen Molecular Ions with Few ppt Uncertainty. *Phys. Rev. Lett.* **2017**, *118*, 233001.

(3) Alighanbari, S.; Giri, G. S.; Constantin, F. L.; Korobov, V. I.; Schiller, S. Precise test of quantum electrodynamics and determination of fundamental constants with HD$^+$ ions. *Nature* **2020**, *581*, 152−158.

(4) Puchalski, M.; Komasa, J.; Pachucki, K. Relativistic corrections for the ground electronic state of molecular hydrogen. *Phys. Rev. A* **2017**, *95*, 052506.

(5) Puchalski, M.; Spyszkiewicz, A.; Komasa, J.; Pachucki, K. Nonadiabatic Relativistic Correction to the Dissociation Energy of H_2, H_2, and HD. *Phys. Rev. Lett.* **2018**, *121*, 073001.

(6) Czachorowski, P.; Puchalski, M.; Komasa, J.; Pachucki, K. Nonadiabatic relativistic correction in H_2, D_2, and HD. *Phys. Rev. A* **2018**, *98*, 052506.

(7) Puchalski, M.; Komasa, J.; Czachorowski, P.; Pachucki, K. Nonadiabatic QED Correction to the Dissociation Energy of the Hydrogen Molecule. *Phys. Rev. Lett.* **2019**, *122*, 103003.

(8) Wang, L. M.; Yan, Z.-C. Relativistic corrections to the ground state of H_2 calculated without using the Born-Oppenheimer approximation. *Phys. Rev. A* **2018**, *97*, 060501.

(9) Cheng, C.-F.; Hussels, J.; Niu, M.; Bethlem, H. L.; Eikema, K. S. E.; Salumbides, E. J.; Ubachs, W.; Beyer, M.; Hölsch, N.; Agner, J. A.; et al. Dissociation Energy of the Hydrogen Molecule at 10^{-9} Accuracy. *Phys. Rev. Lett.* **2018**, *121*, 013001.

(10) Beyer, M.; Hölsch, N.; Hussels, J.; Cheng, C.-F.; Salumbides, E. J.; Eikema, K. S. E.; Ubachs, W.; Jungen, C.; Merkt, F. Determination of the Interval between the Ground States of Para- and Ortho-H_2. *Phys. Rev. Lett.* **2019**, *123*, 163002.

(11) Pachucki, K.; Komasa, J. Nonrelativistic energy of tritium-containing hydrogen molecule isotopologues. *Mol. Phys.* **2022**, *120*, No. e2040627.

(12) Pachucki, K.; Komasa, J. Relativistic Correction from the Four-Body Nonadiabatic Exponential Wave Function. *J. Chem. Theory Comput.* **2024**, *20*, 8644−8651.

(13) Kinghorn, D. B.; Adamowicz, L. Improved Nonadiabatic Ground-State Energy Upper Bound for Dihydrogen. *Phys. Rev. Lett.* **1999**, *83*, 2541−2543.

(14) Kinghorn, D. B.; Adamowicz, L. High accuracy non-Born−Oppenheimer calculations for the isotopomers of the hydrogen

molecule with explicitly correlated Gaussian functions. *J. Chem. Phys.* **2000**, *113*, 4203−4205.

(15) Scheu, C. E.; Kinghorn, D. B.; Adamowicz, L. Non-Born−Oppenheimer calculations on the LiH molecule with explicitly correlated Gaussian functions. *J. Chem. Phys.* **2001**, *114*, 3393−3397.

(16) Bubin, S.; Adamowicz, L. Variational calculations of excited states with zero total angular momentum (vibrational spectrum) of H_2 without use of the Born−Oppenheimer approximation. *J. Chem. Phys.* **2003**, *118*, 3079−3082.

(17) Bubin, S.; Adamowicz, L. Nonrelativistic molecular quantum mechanics without approximations: Electron affinities of LiH and LiD. *J. Chem. Phys.* **2004**, *121*, 6249−6253.

(18) Bubin, S.; Adamowicz, L.; Molski, M. An accurate non-Born−Oppenheimer calculation of the first purely vibrational transition in LiH molecule. *J. Chem. Phys.* **2005**, *123*, 134310.

(19) Bubin, S.; Adamowicz, L. Non-Born-Oppenheimer variational calculation of the ground-state vibrational spectrum of LiH^+. *J. Chem. Phys.* **2006**, *125*, 064309.

(20) Bubin, S.; Adamowicz, L. Calculations of the ground states of BeH and BeH^+ without the Born-Oppenheimer approximation. *J. Chem. Phys.* **2007**, *126*, 214305.

(21) Bubin, S.; Stanke, M.; Adamowicz, L. Non-Born−Oppenheimer calculations of the BH molecule. *J. Chem. Phys.* **2009**, *131*, 044128.

(22) Stanke, M.; Bubin, S.; Adamowicz, L. Fundamental vibrational transitions of the $^3He^4He^+$ and $^7LiH^+$ ions calculated without assuming the Born-Oppenheimer approximation and with including leading relativistic corrections. *Phys. Rev. A* **2009**, *79*, 060501.

(23) Nasiri, S.; Adamowicz, L.; Bubin, S. Electron affinity of $LiH^−$. *Mol. Phys.* **2022**, *120*, No. e2065375.

(24) Nasiri, S.; Shomenov, T.; Bubin, S.; Adamowicz, L. Dissociation energy and the lowest vibrational transition in LiH without assuming the non-Born−Oppenheimer approximation. *Mol. Phys.* **2022**, *120*, No. e2147105.

(25) Nasiri, S.; Bubin, S.; Stanke, M.; Adamowicz, L. Molecular Structure Theory Without the Born−Oppenheimer Approximation: Rotationless Vibrational States of LiH. *J. Phys. Chem. A* **2024**, *128*, 9175−9183.

(26) Adamowicz, L.; Stanke, M.; Tellgren, E.; Helgaker, T. A quantum-mechanical non-Born−Oppenheimer model of a molecule in a strong magnetic field. *Chem. Phys. Lett.* **2020**, *761*, 138041.

(27) Adamowicz, L.; Stanke, M.; Tellgren, E.; Helgaker, T. A computational quantum-mechanical model of a molecular magnetic trap. *J. Chem. Phys.* **2018**, *149*, 244112.

(28) Adamowicz, L.; Stanke, M.; Tellgren, E.; Helgaker, T. Explicitly-correlated non-born-Oppenheimer calculations of the HD molecule in a strong magnetic field. *Chem. Phys. Lett.* **2017**, *682*, 87−90.

(29) Adamowicz, L.; Tellgren, E. I.; Helgaker, T. Non-Born-Oppenheimer calculations of the HD molecule in a strong magnetic field. *Chem. Phys. Lett.* **2015**, *639*, 295−299.

(30) Woźniak, A. P.; Adamowicz, L.; Pedersen, T. B.; Kvaal, S. Gaussian for Electronic and Rovibrational Quantum Dynamics. *J. Phys. Chem. A* **2024**, *128*, 3659−3671.

(31) Adamowicz, L.; Kvaal, S.; Lasser, C.; Pedersen, T. B. Laser-induced dynamic alignment of the HD molecule without the Born−Oppenheimer approximation. *J. Chem. Phys.* **2022**, *157*, 144302.

(32) Wang, M.; Huang, W.; Kondev, F.; Audi, G.; Naimi, S. The AME 2020 atomic mass evaluation (II). Tables, graphs and references. *Chin. Phys. C* **2021**, *45*, 030003.

(33) Bubin, S.; Adamowicz, L. Matrix elements of *N*-particle explicitly correlated Gaussian basis functions with complex exponential parameters. *J. Chem. Phys.* **2006**, *124*, 224317.

(34) Bubin, S.; Adamowicz, L. Energy and energy gradient matrix elements with *N*-particle explicitly correlated complex Gaussian basis functions with $L = 1$. *J. Chem. Phys.* **2008**, *128*, 114107.

(35) Matsen, F. A.; Pauncz, R. *The Unitary Group in Quantum Chemistry*; Elsevier: Amsterdam, 1986.

(36) Pauncz, R. *Spin Eigenfunctions*; Plenum: New York, 1979.

(37) Hamermesh, M. *Group Theory and Its Application to Physical Problems*; Addison-Wesley: Reading, MA, 1962.

(38) Caswell, W. E.; Lepage, G. P. Effective Lagrangians for bound state problems in QED, QCD, and other field theories. *Phys. Lett. B* **1986**, *167*, 437−442.

(39) Pachucki, K. Effective Hamiltonian approach to the bound state: Positronium hyperfine structure. *Phys. Rev. A* **1997**, *56*, 297−304.

(40) Bethe, H. A.; Salpeter, E. E. *Quantum Mechanics of One- and Two-Electron Atoms*; Plenum: New York, 1977.

(41) Akhiezer, A. I.; Berestetskii, V. B. *Quantum Electrodynamics*; John Wiley & Sons: New York, 1965.

(42) Bubin, S.; Stanke, M.; Molski, M.; Adamowicz, L. Accurate non-Born-Oppenheimer calculations of the lowest vibrational energies of D_2 and T_2 with including relativistic corrections. *Chem. Phys. Lett.* **2010**, *494*, 21−25.

(43) Bubin, S.; Pavanello, M.; Tung, W.-C.; Sharkey, K. L.; Adamowicz, L. Born−Oppenheimer and Non-Born−Oppenheimer, Atomic and Molecular Calculations with Explicitly Correlated Gaussian. *Chem. Rev.* **2013**, *113*, 36−79.

(44) Kędziorski, A.; Stanke, M.; Adamowicz, L. Atomic fine-structure calculations performed with a finite-nuclear-mass approach and with all-electron explicitly correlated Gaussian functions. *Chem. Phys. Lett.* **2020**, *751*, 137476.

(45) Tiesinga, E.; Mohr, P. J.; Newell, D. B.; Taylor, B. N. CODATA recommended values of the fundamental physical constants: 2018. *Rev. Mod. Phys.* **2021**, *93*, 025010.

(46) Stanke, M.; Kędziorski, A.; Nasiri, S.; Adamowicz, L.; Bubin, S. Fine structure of the ^2P energy levels of singly ionized carbon (C II). *Phys. Rev. A* **2023**, *108*, 012812.

(47) Pachucki, K.; Komasa, J. Bethe logarithm for the lithium atom from exponentially correlated Gaussian functions. *Phys. Rev. A* **2003**, *68*, 042507.

(48) Pachucki, K.; Komasa, J. Relativistic and QED Corrections for the Beryllium Atom. *Phys. Rev. Lett.* **2004**, *92*, 213001.

(49) Palikot, E.; Stanke, M.; Adamowicz, L. An algorithm for calculating the Bethe logarithm for small molecules with all-electron explicitly correlated Gaussian functions. *Chem. Phys. Lett.* **2020**, *757*, 137859.

(50) Ferenc, D.; Mátyus, E. Evaluation of the Bethe Logarithm: From Atom to Chemical Reaction. *J. Phys. Chem. A* **2023**, *127*, 627−633.

(51) Lesiuk, M.; Lang, J. Atomic Bethe logarithm in the mean-field approximation. *Phys. Rev. A* **2023**, *108*, 042817.

(52) Puchalski, M.; Komasa, J.; Pachucki, K. Explicitly correlated wave function for a boron atom. *Phys. Rev. A* **2015**, *92*, 062501.

(53) Bubin, S.; Komasa, J.; Stanke, M.; Adamowicz, L. Isotope shifts of the three lowest ^1S states of the B^+ ion calculated with a finite-nuclear-mass approach and with relativistic and quantum electrodynamics corrections. *J. Chem. Phys.* **2010**, *132*, 114109.

(54) Drake, G. W. F.; Swainson, R. A. Bethe logarithms for hydrogen up to $n = 20$, and approximations for two-electron atoms. *Phys. Rev. A* **1990**, *41*, 1243−1246.

(55) Drachman, R. J. A new global operator for two-particle delta functions. *J. Phys. B* **1981**, *14*, 2733.

(56) Hornyák, I.; Adamowicz, L.; Bubin, S. Low-lying ^2S states of the singly charged carbon ion. *Phys. Rev. A* **2020**, *102*, 062825.

(57) Nasiri, S.; Shomenov, T.; Bubin, S.; Adamowicz, L. High-accuracy calculations of the lowest eleven Rydberg ^2P states of Li atom. *J. Phys. B* **2021**, *54*, 085003.

(58) Miliordos, E.; Mavridis, A. Ab initio investigation of the electronic structure and bonding of BH, $BH^−$, and HBBH molecules. *J. Chem. Phys.* **2008**, *128*, 144308.

(59) Viteri, C. R.; Gilkison, A. T.; Rixon, S. J.; Grant, E. R. Rovibrational characterization of $X^2\Sigma^{+11}BH^+$ by the extrapolation of photoselected high Rydberg series in ^{11}BH. *J. Chem. Phys.* **2006**, *124*, 144312.

(60) Valeev, E. F.; Sherrill, C. D. The diagonal Born−Oppenheimer correction beyond the Hartree−Fock approximation. *J. Chem. Phys.* **2003**, *118*, 3921−3927.

(61) Feller, D.; Dixon, D. A.; Peterson, K. A. Heats of Formation of Simple Boron Compounds. *J. Phys. Chem. A* **1998**, *102*, 7053−7059.

(62) Johnson, R. D. *Computational Chemistry Comparison and Benchmark Database, Number 101*; NIST, 2022; ..

(63) Bauer, S. H.; Herzberg, G.; Johns, J. W. C. The absorption spectrum of BH and BD in the vacuum ultraviolet. *J. Mol. Spectrosc.* **1964**, *13*, 256−280.

(64) Huber, K. P.; Herzberg, G. *Molecular spectra and molecular structure: IV. Constants of diatomic molecules*; Springer Science & Business Media, 1979.

(65) Koput, J. Ab Initio spectroscopic characterization of borane, BH, in its electronic state. *J. Comput. Chem.* **2015**, *36*, 2219−2227.

(66) Petsalakis, I. D.; Theodorakopoulos, G. Theoretical study of nonadiabatic interactions, radiative lifetimes and predissociation lifetimes of excited states of BH. *Mol. Phys.* **2007**, *105*, 333−342.

(67) Johns, J. W. C.; Grimm, F. A.; Porter, R. F. On the spectrum of BH in the near ultraviolet. *J. Mol. Spectrosc.* **1967**, *22*, 435−451.

(68) Bauschlicher, C. W.; Langhoff, S. R.; Taylor, P. R. On the dissociation energy of BH. *J. Chem. Phys.* **1990**, *93*, 502−506.

(69) Shi, D.-H.; Liu, H.; Zhang, J.-P.; Sun, J.-F.; Liu, Y.-F.; Zhu, Z.-L. Spectroscopic investigations on $BH^+(X^2\Sigma^+)$ ion using MRCI method and correlation-consistent sextuple basis set augmented with diffuse functions. *Int. J. Quantum Chem.* **2011**, *111*, 2171−2179.

(70) Hornyák, I.; Nasiri, S.; Bubin, S.; Adamowicz, L. ^2S Rydberg spectrum of the boron atom. *Phys. Rev. A* **2021**, *104*, 032809.

(71) Nasiri, S.; Tumakov, D.; Stanke, M.; Kędziorski, A.; Adamowicz, L.; Bubin, S. Fine structure of the doublet *P* levels of boron. *Phys. Rev. Research* **2024**, *6*, 043225.

(72) Martin, J. M. Benchmark ab initio potential curves for the light diatomic hydrides. Unusually large nonadiabatic effects in BeH and BH. *Chem. Phys. Lett.* **1998**, *283*, 283−293.

(73) Pachucki, K.; Cencek, W.; Komasa, J. On the acceleration of the convergence of singular operators in Gaussian basis sets. *J. Chem. Phys.* **2005**, *122*, 184101.

(74) Cioslowski, J.; Strasburger, K. Plain Capping for Improved Accuracy of Approximate One- and Two-Electron Densities at Two-Particle Coalescence Points. *J. Chem. Theory Comput.* **2024**, *20*, 7876−7883.

(75) Jeszenszki, P.; Ireland, R. T.; Ferenc, D.; Mátyus, E. On the inclusion of cusp effects in expectation values with explicitly correlated Gaussian. *Int. J. Quantum Chem.* **2022**, *122*, No. e26819.

(76) Rácsai, B.; Ferenc, D.; Margócsy, Á.; Mátyus, E. Regularized relativistic corrections for polyelectronic and polyatomic systems with explicitly correlated Gaussian. *J. Chem. Phys.* **2024**, *160*, 211102.

(77) Le Roy, R. J. LEVEL: A computer program for solving the radial Schrödinger equation for bound and quasibound levels. *J. Quant. Spectrosc. Radiat. Transfer* **2017**, *186*, 167−178.